Contents lists available at ScienceDirect

Physics Letters B

www.elsevier.com/locate/physletb

PHYSICS LETTERS B

Decay constants of pseudoscalar D-mesons in lattice QCD with domain-wall fermion

CrossMark

TWQCD Collaboration

Wen-Ping Chen [a], Yu-Chih Chen [a], Ting-Wai Chiu [a,b,*], Han-Yi Chou [a], Tian-Shin Guu [c], Tung-Han Hsieh [d]

[a] *Physics Department, National Taiwan University, Taipei 10617, Taiwan*
[b] *Center for Quantum Science and Engineering, National Taiwan University, Taipei 10617, Taiwan*
[c] *Center for Science Education, National Ilan University, I-Lan 260, Taiwan*
[d] *Research Center for Applied Sciences, Academia Sinica, Taipei 115, Taiwan*

A R T I C L E   I N F O

A B S T R A C T

We present the first study of the masses and decay constants of the pseudoscalar D mesons in two flavors lattice QCD with domain-wall fermion. The gauge ensembles are generated on the $24^3 \times 48$ lattice with the extent $N_s = 16$ in the fifth dimension, and the plaquette gauge action at $\beta = 6.10$, for three sea-quark masses with corresponding pion masses in the range 260–475 MeV. We compute the point-to-point quark propagators, and measure the time-correlation functions of the pseudoscalar and vector mesons. The inverse lattice spacing is determined by the Wilson flow, while the strange and the charm quark masses by the masses of the vector mesons $\phi(1020)$ and $J/\psi(3097)$ respectively. Using heavy meson chiral perturbation theory (HMChPT) to extrapolate to the physical pion mass, we obtain $f_D = 202.3(2.2)(2.6)$ MeV and $f_{D_s} = 258.7(1.1)(2.9)$ MeV.

In the Standard Model (SM), the quark and antiquark of a charged pseudoscalar meson P (with quark content $Q\bar{q}$) can decay into a charged lepton and its associated neutrino through a virtual W boson. This is the purely leptonic decay of the charged pseudoscalar meson. To the lowest order, the purely leptonic decay width can be written as

$$\Gamma(P \to l\nu) = \frac{G_F^2}{8\pi}|V_{Qq}|^2 m_l^2 \left(1 - \frac{m_l^2}{M_P^2}\right)^2 M_P f_P^2, \qquad (1)$$

where G_F is the Fermi coupling constant, V_{Qq} is the Cabibbo–Kobayashi–Maskawa (CKM) matrix element, m_l is the mass of the lepton, M_P is the mass of the charged pseudoscalar meson, and f_P is the decay constant of the charged pseudoscalar meson, which is defined by the matrix element of the axial vector current between the QCD vacuum and the one-particle state of the charged pseudoscalar meson,

$$\langle 0|\bar{q}\gamma_\mu\gamma_5 Q(0)|P(\vec{q})\rangle = if_P q_\mu. \qquad (2)$$

According to (1), experimental measurement of the leptonic decay width gives a determination of the product $|V_{Qq}|f_P$. If the value of

f_P can be obtained from another experimental measurement, then the value of $|V_{Qq}|$ can be determined, which is crucial for testing the SM via the unitarity of the CKM matrix, as a constraint for any new physics beyond the SM. On the other hand, if the value of f_P is unavailable from other experiments, then it must be determined theoretically from the first principles of QCD, before the value of $|V_{Qq}|$ can be fixed.

Theoretically, lattice QCD is a viable framework to tackle QCD nonperturbatively from the first principles of QCD, by discretizing the continuum space–time on a 4-dimensional space–time lattice [1], and computing physical observables by Monte Carlo simulation [2]. However, in practice, any lattice QCD calculation suffers from the discretization and finite volume errors, plus the systematic error due to the unphysically heavy u/d quark masses (with $M_\pi > 140$ MeV). Moreover, since all quarks in QCD are excitations of Dirac fermion fields, it is vital to preserve all salient features of the Dirac fermion field on the lattice, in particular, the chiral symmetry of the massless Dirac fermion field. It is nontrivial to formulate Dirac fermion field with exact chiral symmetry at finite lattice spacing. This is realized through the domain-wall fermion (DWF) on the 5-dimensional lattice [3] and the overlap-Dirac fermion on the 4-dimensional lattice [4].

* Corresponding author.
  E-mail address: twchiu@phys.ntu.edu.tw (T.-W. Chiu).

In June 2005, we determined the masses and decay constants of pseudoscalar mesons D and D_s in quenched lattice QCD with exact chiral symmetry [5], before the CLEO Collaboration announced their high-statistics measurement of f_D in July 2005. Our theoretical predictions of f_D and f_{D_s} turned out in good agreement with the experimental values from the CLEO Collaboration [6,7]. In 2007, we extended our study to the B-mesons [8], and determined the masses and decay constants of B_s and B_c, as well as the lowest-lying spectra of heavy mesons with quark contents $b\bar{b}$, $c\bar{b}$, $s\bar{b}$, and $c\bar{c}$.

To remove the systematic error due to the quenched approximation, it is necessary to simulate lattice QCD with dynamical quarks. For lattice QCD with exact chiral symmetry, the challenge is how to perform the hybrid Monte Carlo (HMC) simulation [9] such that the chiral symmetry is preserved at a high precision and all topological sectors are sampled ergodically.

During 2011–2012, we demonstrated that it is feasible to perform large-scale dynamical QCD simulations with the optimal domain-wall fermion (ODWF) [10], which not only preserves the chiral symmetry to a good precision, but also samples all topological sectors ergodically. To recap, we perform HMC simulations of two flavors QCD on the $16^3 \times 32$ lattice (with lattice spacing $a \sim 0.1$ fm), for eight sea-quark masses corresponding to the pion masses in the range 228–565 MeV. Our results of the topological susceptibility [11], as well as the mass and decay constant of the pseudoscalar meson [12], are all in good agreement with the sea-quark mass dependence predicted by the next-to-leading order (NLO) chiral perturbation theory (ChPT). This asserts that the nonperturbative chiral dynamics of the sea-quarks are well under control in our HMC simulations. In this paper, we perform HMC simulations of two flavors QCD with ODWF on the $24^3 \times 48$ lattice (with lattice spacing $a \sim 0.062$ fm), with the purpose of studying the charm physics in lattice QCD with exact chiral symmetry.

In general, the 5-dimensional lattice Dirac operator of ODWF can be written as [13]

$$[\mathcal{D}(m)]_{xx';ss'} = (\rho_s D_w + 1)_{xx'}\delta_{ss'} + (\sigma_s D_w - 1)_{xx'}L_{ss'}, \quad (3)$$

where $\rho_s = c\omega_s + d$, $\sigma_s = c\omega_s - d$, and c, d are constants. The indices x and x' denote the sites on the 4-dimensional space–time lattice, and s and s' the indices in the fifth dimension, while the lattice spacing a and the Dirac and color indices have been suppressed. The weights $\{\omega_s, \ s = 1, \ldots, N_s\}$ along the fifth dimension are fixed according to the formula derived in [10] such that the maximal chiral symmetry is attained. Here D_w is the standard Wilson Dirac operator plus a negative parameter $-m_0$ ($0 < m_0 < 2$),

$$(D_w)_{xx'} = -\frac{1}{2}\sum_\mu \left[(1 - \gamma_\mu)U_\mu(x)\delta_{x+\hat{\mu},x'} \right.$$
$$\left. + (1 + \gamma_\mu)U_\mu^\dagger(x')\delta_{x-\hat{\mu},x'} \right] + (4 - m_0), \quad (4)$$

where $U_\mu(x)$ denotes the link variable pointing from x to $x + \hat{\mu}$. The operator L is independent of the gauge field, and it can be written as

$$L = P_+L_+ + P_-L_-, \quad P_\pm = (1 \pm \gamma_5)/2,$$

and

$$(L_+)_{ss'} = (L_-)_{s's} = \begin{cases} -m\delta_{N_s,s'}, & s = 1, \\ \delta_{s-1,s'}, & 1 < s \le N_s, \end{cases}$$

where N_s is the number of sites in the fifth dimension, $m \equiv rm_q$, m_q is the bare quark mass, and $r = 1/[2m_0(1 - dm_0)]$.

Including the action of Pauli–Villars fields (with bare mass $m_{PV} = 1/r$), the partition function of ODWF in a gauge background can be written as

$$Z_{odwf} = \int [d\Psi][d\bar{\Psi}][d\Phi][d\Phi^\dagger] \exp\{-\bar{\Psi}\mathcal{D}(m)\Psi - \Phi^\dagger\mathcal{D}(1)\Phi\}, \quad (5)$$

which can be integrated successively to obtain the fermion determinant of the effective 4-dimensional Dirac operator [10]

$$Z_{odwf} = \det D(m_q), \quad D(m_q) = (D_c + m_q)(1 + rD_c)^{-1}, \quad (6)$$

where

$$D_c = \frac{1}{r}\frac{1 + \gamma_5 S_{opt}(H)}{1 - \gamma_5 S_{opt}(H)}, \quad S_{opt}(H) = \frac{1 - \prod_{s=1}^{N_s} T_s}{1 + \prod_{s=1}^{N_s} T_s},$$

$$T_s = \frac{1 - \omega_s H}{1 + \omega_s H}, \quad H = cH_w(1 + d\gamma_5 H_w)^{-1},$$

$$H_w = \gamma_5 D_w(-m_0). \quad (7)$$

Here $S_{opt}(H) = HR_Z(H)$, where $R_Z(H)$ is the Zolotarev optimal rational approximation of $(H^2)^{-1/2}$.

For HMC simulation of lattice QCD with ODWF, it is crucial to perform the even–odd preconditioning on the ODWF operator (3) such that the condition number of the conjugate gradient is reduced and the memory consumption is halved. Now, separating the even and the odd sites on the 4-dimensional space–time lattice, (3) can be written as

$$\mathcal{D}(m_q) = \begin{pmatrix} 4 - m_0 & D_w^{EO} \\ D_w^{OE} & 4 - m_0 \end{pmatrix}[c\omega(1 + L) + d(1 - L)] + (1 - L)$$
$$= \begin{pmatrix} X & D_w^{EO}Y \\ D_w^{OE}Y & X \end{pmatrix}, \quad (8)$$

where

$$X \equiv (4 - m_0)[c\omega(1 + L) + d(1 - L)] + (1 - L),$$
$$Y \equiv c\omega(1 + L) + d(1 - L). \quad (9)$$

We further rewrite it in a more symmetric form by defining

$$M_5 \equiv \omega^{-1/2}YX^{-1}\omega^{1/2}$$
$$= \left\{(4 - m_0) + \omega^{-1/2}[c(1 + L)(1 - L)^{-1} + d\omega^{-1}]^{-1}\omega^{-1/2}\right\}^{-1}, \quad (10)$$

and

$$S_1 \equiv \omega^{-1/2}YX^{-1} = M_5\omega^{-1/2}, \quad S_2 \equiv Y^{-1}\omega^{1/2}. \quad (11)$$

Then Eq. (8) becomes

$$\mathcal{D}(m_q) = S_1^{-1}\begin{pmatrix} 1 & M_5 D_w^{EO} \\ M_5 D_w^{OE} & 1 \end{pmatrix}S_2^{-1}$$
$$= S_1^{-1}\begin{pmatrix} 1 & 0 \\ M_5 D_w^{OE} & 1 \end{pmatrix}\begin{pmatrix} 1 & 0 \\ 0 & C \end{pmatrix}\begin{pmatrix} 1 & M_5 D_w^{EO} \\ 0 & 1 \end{pmatrix}S_2^{-1}, \quad (12)$$

where the Schur decomposition has been used in the last equality, with the Schur complement

$$C \equiv 1 - M_5 D_w^{OE}M_5 D_w^{EO}. \quad (13)$$

Since $\det \mathcal{D} = \det S_1^{-1} \cdot \det C \cdot \det S_2^{-1}$, and S_1 and S_2 do not depend on the gauge field, we can just use C for the Monte Carlo simulation. After including the Pauli–Villars fields (with $m_{PV} = 1/r$), the pseudofermion action for two-flavors QCD (in the isospin symmetry limit $m_u = m_d$) can be written as

$$S_{pf} = \phi^\dagger C_1^\dagger(CC^\dagger)^{-1}C_1\phi, \quad C_1 \equiv C(m = 1), \quad (14)$$

where ϕ and $\phi^\dagger$ are complex scalar fields carrying the same quantum numbers (color, spin) of the quark fields. Including the gluon fields, the partition function for 2 flavors QCD can be written as

$$Z = \int [dU][d\phi^\dagger][d\phi] \exp\left(-S_g[U] - \phi^\dagger C_1^\dagger (CC^\dagger)^{-1} C_1 \phi\right), \quad (15)$$

where $S_g[U]$ is the lattice action for the gluon field. Here we use the plaquette gauge action

$$S_g[U] = \beta \sum_{plaq.} \left\{ 1 - \frac{1}{3} \operatorname{Re} \operatorname{Tr}(U_p) \right\}, \quad \beta = \frac{6}{g^2}. \quad (16)$$

Further details of our HMC simulations of two flavors QCD can be found in Ref. [14] and a forthcoming long paper.

We perform the hybrid Monte Carlo simulation of two flavors QCD on the $24^3 \times 48$ lattice with the plaquette gauge action at $\beta = 6/g^2 = 6.10$, for three sea-quark masses ($m_{sea}a = 0.005, 0.01, 0.02$) with the corresponding pion masses in the range 260–475 MeV. For the quark part, we use ODWF with $c = 1$, $d = 0$ (i.e., $H = H_w$), $N_s = 16$, and $\lambda_{\min}/\lambda_{\max} = 0.05/6.2$. For each sea-quark mass, we generate the initial 400–500 trajectories on an Nvidia GPU card (with device memory larger than 4 GB). After discarding initial 300 trajectories for thermalization, we sample one configuration every 5 trajectories, resulting 20–32 "seed" configurations for each sea-quark mass. Then we use these seed configurations as the initial configurations for independent simulations on 20–32 GPUs. Each GPU generates 200–250 trajectories independently. Then we accumulate a total of 5000 trajectories for each sea-quark mass. From the saturation of the binning error of the plaquette, as well as the evolution of the topological charge, we estimate the autocorrelation time to be around 10 trajectories. Thus we sample one configuration every 10 trajectories, and obtain ~500 configurations for each ensemble. The basic parameters of these three ensembles are summarized in Table 1.

In Fig. 1, we plot the histogram of the topological charge (Q_t) distribution for these three ensembles. Evidently, the probability distribution of Q_t for each ensemble behaves like a Gaussian, and it becomes more sharply peaked around $Q_t = 0$ as the sea-quark mass gets smaller. Here the topological charge $Q_t = \sum_x \epsilon_{\mu\nu\lambda\sigma} \operatorname{tr}[F_{\mu\nu}(x) F_{\lambda\sigma}(x)]/(32\pi^2)$, where the matrix-valued field tensor $F_{\mu\nu}(x)$ is obtained from the four plaquettes surrounding x

Table 1
Basic parameters of the gauge ensembles: the sea-quark mass, the number of gauge configurations in each ensemble, the inverse lattice spacing, the residual mass, and the pion mass.

Ensemble	$m_{sea}a$	N_{cfg}	a^{-1} [GeV]	$m_{res}a$	M_π [MeV]
A	0.005	535	3.194(11)(12)	0.000057(5)	259(10)(11)
B	0.010	506	3.138(16)(12)	0.000046(4)	347(7)(6)
C	0.020	501	3.044(13)(11)	0.000028(3)	474(6)(5)

on the $(\hat{\mu}, \hat{\nu})$ plane. Even though the resulting topological charge is not exactly equal to an integer, the probability distribution $P(Q_t)$ suffices to demonstrate that our HMC simulation indeed samples all topological sectors ergodically. For a rigorous study of topology, we are projecting the zero modes and the low-lying eigenmodes of the overlap Dirac operator for each gauge configuration, with the same procedures as outlined in Ref. [11], and we will report our results in a forthcoming long paper.

To determine the lattice scale, we use the Wilson flow [15] with the condition [16]

$$\left\{ t^2 \langle E(t) \rangle \right\}\big|_{t=t_0} = 0.3 \quad (17)$$

to obtain $\sqrt{t_0}/a$ for each gauge ensemble. Our procedures are as follows. First, we compute the Wilson flow for each gauge ensemble of the 2-flavors QCD on the $16^3 \times 32$ lattice at $\beta = 5.95$ [12], and obtain the value of $\sqrt{t_0}/a$. By linear extrapolation, we obtain $\sqrt{t_0}/a = 1.3674(67)(42)$ in the chiral limit, where the systematic error is estimated by varying the number of sea-quark masses used for the linear extrapolation. Then, using the lattice spacing $a = 0.1034(1)(2)$ fm (in the chiral limit) [12] which has been determined at $\beta = 5.95$ (by heavy quark potential with Sommer parameter $r_0 = 0.49$ fm), we obtain $\sqrt{t_0} = 0.1414(7)(5)$ fm. Thus, with the input $\sqrt{t_0} = 0.1414(7)(5)$ fm, we can determine the lattice spacing of any gauge ensemble of 2-flavors QCD, with the value of $\sqrt{t_0}/a$ obtained by the Wilson flow with the condition (17). For the gauge ensembles of 2-flavors QCD on the $24^3 \times 48$ lattice at $\beta = 6.10$, a^{-1} [GeV] $= 3.194(11)(12), 3.138(16)(12)$, $3.044(13)(11)$, for $m_{sea}a = 0.005, 0.01$, and 0.02 respectively. The inverse lattice spacing is well fitted by the linear function of $m_{sea}a$, which gives $a^{-1} = 3.2418(35)(44)$ GeV in the chiral limit.

We compute the valence quark propagator with the point source at the origin, and with parameters exactly the same as
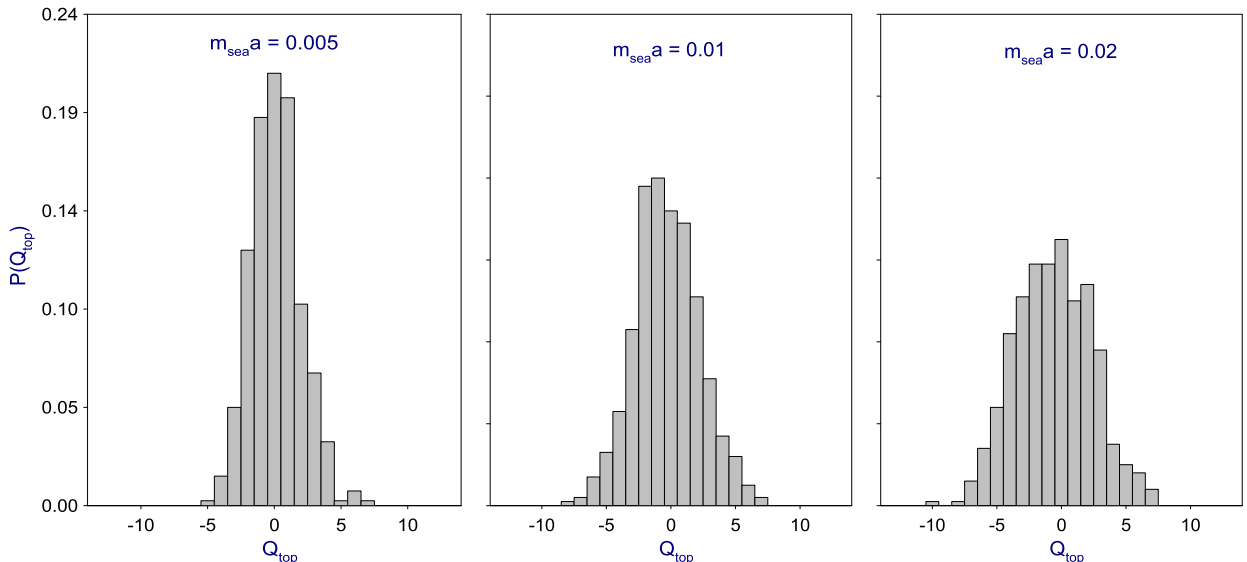

Fig. 1. Histogram of topological charge distribution for three sea-quark masses, $m_{sea}a = 0.005, 0.01$, and 0.02 respectively.

Table 2
Determination of the strange quark and the charm quark masses.

Ensemble	$m_s a$	M_ϕ [MeV]	$[t_1, t_2]$	χ^2/dof	$m_c a$	$M_{J/\psi}$ [MeV]	$[t_1, t_2]$	χ^2/dof
A	0.04	1020(7)	[11, 24]	0.99	0.53	3097(11)	[15, 24]	0.25
B	0.04	1020(8)	[11, 23]	0.11	0.55	3104(15)	[17, 23]	0.58
C	0.04	1020(8)	[16, 23]	0.20	0.55	3099(13)	[16, 24]	0.22

Table 3
The mass and decay constant of D-mesons.

Ensemble	M_D [MeV]	f_D [MeV]	$[t_1, t_2]$	χ^2/dof	M_{D_s} [MeV]	f_{D_s} [MeV]	$[t_1, t_2]$	χ^2/dof
A	1862(11)	216(5)	[17, 24]	0.83	1969(8)	261(5)	[14, 23]	0.97
B	1864(10)	220(4)	[18, 23]	0.82	1968(9)	264(4)	[13, 24]	0.54
C	1877(10)	227(6)	[18, 22]	0.54	1962(8)	267(3)	[10, 17]	0.70

those of the sea-quarks ($N_s = 16$ and $\lambda_{\min}/\lambda_{\max} = 0.05/6.2$). First, we solve the following linear system (with even–odd preconditioned CG),

$$\mathcal{D}(m_q)|Y\rangle = \mathcal{D}(m_{PV})B^{-1}|\text{source vector}\rangle, \tag{18}$$

where $B^{-1}_{x,s;x',s'} = \delta_{x,x'}(P_-\delta_{s,s'} + P_+\delta_{s+1,s'})$ with periodic boundary conditions in the fifth dimension. Then the solution of (18) gives the valence quark propagator

$$(D_c + m_q)^{-1}_{x,x'} = r(1 - r m_q)^{-1}\big[(BY)_{x,1;x',1} - \delta_{x,x'}\big].$$

For each gauge ensemble, we measure the time-correlation functions for pseudoscalar (P) and vector (V) mesons,

$$C_P(t) = \left\langle \sum_{\vec{x}} \text{tr}\big\{\gamma_5(D_c + m_Q)^{-1}_{x,0}\gamma_5(D_c + m_q)^{-1}_{0,x}\big\}\right\rangle_U,$$

$$C_V(t) = \left\langle \frac{1}{3}\sum_{\mu=1}^{3}\sum_{\vec{x}} \text{tr}\big\{\gamma_\mu(D_c + m_Q)^{-1}_{x,0}\gamma_\mu(D_c + m_q)^{-1}_{0,x}\big\}\right\rangle_U,$$

for the following quark contents: $(m_q, m_Q) = \{(m_{sea}, m_{sea}), (m_{sea}, m_s), (m_{sea}, m_c), (m_s, m_s), (m_s, m_c), (m_c, m_c)\}$, where m_s and m_c are the bare masses of the strange quark and the charm quark.

In general, the decay constant f_P of a charged pseudoscalar meson P with quark content $Q\bar{q}$ is defined by (2). In lattice QCD with exact chiral symmetry, we can use the axial Ward identity

$$\partial_\mu(\bar{q}\gamma_\mu\gamma_5 Q) = (m_q + m_Q)\bar{q}\gamma_5 Q$$

to obtain

$$f_P = (m_q + m_Q)\frac{|\langle 0|\bar{q}\gamma_5 Q|P(\vec{0})\rangle|}{M_P^2}, \tag{19}$$

where the pseudoscalar mass $M_P a$ and the decay amplitude $z \equiv |\langle 0|\bar{q}\gamma_5 Q|P(\vec{0})\rangle|$ can be obtained by fitting the pseudoscalar time-correlation function $C_P(t)$ to the formula

$$\frac{z^2}{2M_P a}\big[e^{-M_P a t} + e^{-M_P a(T-t)}\big], \tag{20}$$

where the excited states have been neglected.

To measure the chiral symmetry breaking due to finite N_s, we compute the residual mass according to the formula [13]

$$m_{res} = \frac{\langle \text{tr}(D_c + m_q)^{-1}_{0,0}\rangle_U}{\langle \text{tr}[\gamma_5(D_c + m_q)\gamma_5(D_c + m_q)]^{-1}_{0,0}\rangle_U} - m_q, \tag{21}$$

where $(D_c + m_q)^{-1}$ denotes the valence quark propagator with m_q equal to the sea-quark mass, tr denotes the trace running over the color and Dirac indices, and the brackets $\langle\cdots\rangle_U$ denote averaging

over an ensemble of gauge configurations. In Table 1, we list the residual mass of each ensemble. We see that the residual mass is at most $\sim$1% of the bare quark mass, amounting to $\sim$0.17 MeV, which is expected to be much smaller than other systematic errors. In Table 1, we list the pion mass which is extracted from the time-correlation function $C_P(t)$ with the valence quark masses equal to the sea-quark mass ($m_q = m_Q = m_{sea}$). Here the pion mass has been corrected for the finite volume effect, using the estimate within ChPT calculated up to $\mathcal{O}(M_\pi^4/(4\pi f_\pi)^4)$ [17].

For each ensemble, the strange quark bare mass m_s is tuned such that the vector-meson mass M_V extracted from the time-correlation function $C_V(t)$ with the valence quark masses $m_q = m_Q = m_s$ is equal to the mass of the vector meson $\phi(1020)$. The vector meson mass M_V is extracted by fitting $C_V(t)$ to a formula similar to (20), for the range $[t_1, t_2]$ in which the effective mass attaining a plateau. We estimate the statistical error of M_V using the jackknife method with the bin size (10–15 configurations) of which the statistical error saturates. To estimate the systematic errors of M_V, besides that due to the systematic error of the inverse lattice spacing (see Table 1), we also incorporate the variation of M_V based on all fittings satisfying χ^2/dof < 1.1. In the following, it is understood that all masses and decay constants, and their errors are obtained with the same procedure. Similarly, the charm quark bare mass m_c is tuned such that the vector-meson mass extracted from the time-correlation function $C_V(t)$ with the valence quark masses $m_q = m_Q = m_c$ is equal to the mass of the vector meson $J/\psi(3097)$. The values of m_s and m_c of each ensemble are summarized in Table 2, where the error denotes the combined statistical and systematic error.

Using the value of m_c in Table 2, we measure the time-correlation function of the D meson with the valence quark masses ($m_q = m_{sea}$, $m_Q = m_c$) for each ensemble. Then we fit the time-correlation function $C_D(t)$ to (20) to extract the D meson mass $M_D a$ and the decay constant $f_D a$. Similarly, using the values of m_s and m_c in Table 2, we measure the time-correlation function of the D_s meson with the valence quark masses ($m_q = m_s$, $m_Q = m_c$), and extract the mass $M_{D_s} a$ and the decay constant $f_{D_s} a$ for each ensemble. Our results of M_D, f_D, M_{D_s}, and f_{D_s} are summarized in Table 3, where the error denotes the combined statistical and systematic error.

We see that for all ensembles, the masses of D and D_s mesons are in good agreement with the experimental values compiled by PDG [18], $M_D = 1869.62 \pm 0.15$ MeV, and $M_{D_s} = 1968.50 \pm 0.32$ MeV.

For the decay constants f_D and f_{D_s}, we use HMChPT [19] to extrapolate to the physical $M_\pi = 140$ MeV. In general, for the pseudoscalar meson with quark content ($c\bar{q}$), the NLO formula for $N_f = 2$ reads
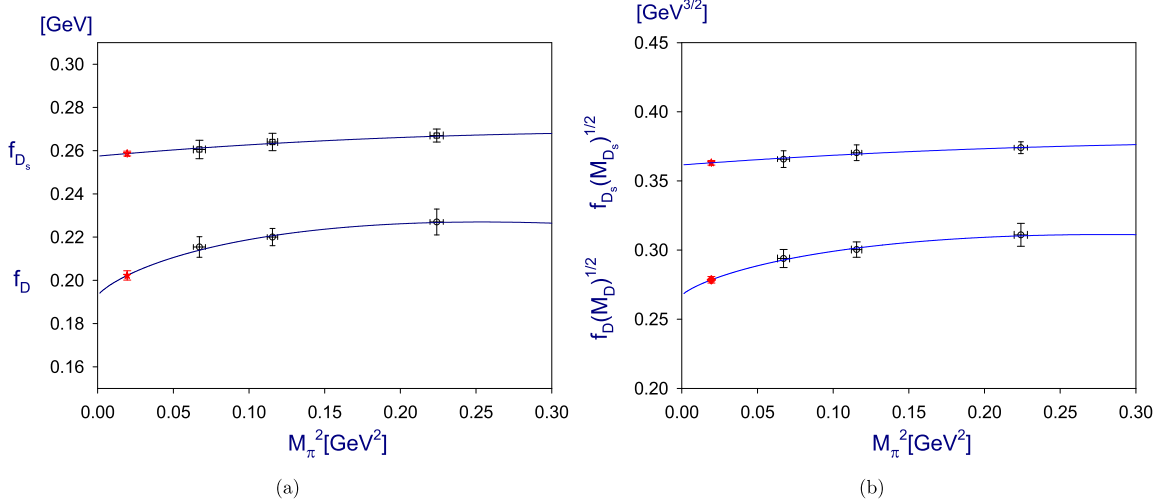
Fig. 2. Fitting the data to NLO HMChPT: (a) f_D and f_{D_s}; (b) $f_D \sqrt{M_D}$ and $f_{D_s} \sqrt{M_{D_s}}$. In each figure, the solid line is the fit of the data points to HMChPT. The symbol (in red) is the extrapolated value at physical $M_\pi = 140$ MeV. (For interpretation of the references to color in this figure legend, the reader is referred to the web version of this article.)

$$f_{D_q} = \frac{\kappa}{\sqrt{M_{D_q}}} \left\{ 1 - \frac{1 + 3g_c^2}{2} \left[(\xi + \xi_q) \ln\left(\frac{\xi + \xi_q}{2} \right) - \frac{\xi_q}{2} \ln \xi_q \right] \right.$$
$$\left. + c_1 \xi \right\}, \tag{22}$$

where $\xi = M_\pi^2 / (4\pi f)^2$, $\xi_q = M_{qq}^2 / (4\pi f)^2$, M_{qq} is the mass of the pseudoscalar meson with quark content $q\bar{q}$, $g_c = 0.61(7)$ which is determined by the experimental measurement of the coupling $g_{D^* \to D\pi}$ [20], and κ and c_1 are low-energy constants. For $\bar{q}$ equal to $\bar{d}$, (22) reduces to

$$f_D = \frac{\kappa}{\sqrt{M_D}} \left[1 - \frac{3}{4} \left(1 + 3g_c^2 \right) \xi \ln \xi + c_1 \xi \right]. \tag{23}$$

Fitting the data of ensembles (A)–(C) to (23) [see the lower curve in Fig. 2(a)], we obtain $\kappa = 0.2638(28)$ and $c_1 = -1.899(206)$ with $\chi^2/\text{dof} = 0.34$. At the physical $M_\pi = 140$ MeV, (23) gives $f_D = 202.3(2.2)$ MeV. Alternatively, performing the fit to $f_D \sqrt{M_D}$ (multiplying both sides of (23) with $\sqrt{M_D}$) [see the lower curve in Fig. 2(b)], we obtain $\kappa = 0.2673(22)$ and $c_1 = -2.012(189)$ with $\chi^2/\text{dof} = 0.27$. At the physical $M_\pi = 140$ MeV, it gives $f_D \sqrt{M_D} = 0.2785(23)$, which in turn (with physical input $M_D = 1869.62$ MeV) yields $f_D = 203.7(1.7)$ MeV. Comparing the results of these two HMChPT fits, we estimate the systematic error of f_D due to the chiral extrapolation to be ~ 1.4 MeV. Next we estimate the systematic error of f_D due to the scaling violations (i.e., the error induced through the scale setting), by performing the chiral extrapolation of $(f_D a) \sqrt{M_D a}$ in the lattice unit, using the raw data of $M_D a$ and $f_D a$ extracted from the time-correlation function. Fitting the lattice data of ensembles (A)–(C) to NLO HMChPT (see the lower curve in Fig. 3) gives $\kappa = 0.0454(2)$ and $c_1 = -0.6923(948)$ with $\chi^2/\text{dof} = 0.14$. At the physical $M_\pi = 140$ MeV ($M_\pi a = 0.001842$), it gives $f_D a \sqrt{M_D a} = 0.0477(2)$. With the inputs $a^{-1} = 3.2418(56)$ GeV (in the chiral limit) and $M_D = 1869.62$ MeV, we obtain $f_D = 203.7(1.0)$ MeV. Thus we estimate the systematic error of f_D due to the scaling violations to be ~ 1.0 MeV. Since our calculation is done at one single lattice spacing, the discretization error cannot be quantified reliably. Nevertheless, we do not expect it to be much larger than the systematic errors due to the chiral extrapolation and the scaling violations, because our lattice action is free from $O(a)$ discretization errors. Now, assuming the discretization error to be ~ 2 MeV,
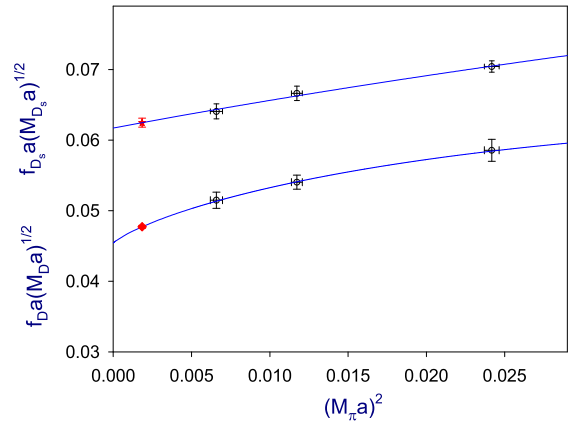

Fig. 3. Fitting the lattice data of $f_D a \sqrt{M_D a}$ and $f_{D_s} a \sqrt{M_{D_s} a}$ (in the lattice unit) to NLO HMChPT. The solid line is the fit to HMChPT, and the symbol (in red) is the extrapolated value at physical $M_\pi = 140$ MeV. (For interpretation of the references to color in this figure legend, the reader is referred to the web version of this article.)

together with the systematic errors due to the scaling violations and the chiral extrapolation, we obtain

$$f_D = 202.3 \pm 2.2 \pm 2.6 \text{ MeV}, \tag{24}$$

which is in good agreement with the experimental values [21,22], as well as the experimental average $f_D = 204.6 \pm 5.0$ MeV [23].

Next, we turn to the decay constant of D_s meson. Fitting the data of ensembles (A)–(C) to (22) with $\bar{q} = \bar{s}$ [see the upper curve in Fig. 2(a)], we obtain $\kappa = 0.2790(12)$ and $c_1 = -0.7740(733)$ with $\chi^2/\text{dof} = 0.20$. At the physical $M_\pi = 140$ MeV, (22) gives $f_{D_s} = 258.7(1.1)$ MeV. Alternatively, performing the fit to $f_{D_s} \sqrt{M_{D_s}}$ [see the upper curve in Fig. 2(b)], we obtain $\kappa = 0.2865(13)$ and $c_1 = -0.8949(899)$ with $\chi^2/\text{dof} = 0.21$. At the physical $M_\pi = 140$ MeV, it gives $f_{D_s} \sqrt{M_{D_s}} = 0.2785(23)$, which (with physical input $M_{D_s} = 1968.50$ MeV) yields $f_{D_s} = 258.8(1.2)$ MeV. Comparing the results of these two HMChPT fits, we estimate the systematic error of f_{D_s} due to the chiral extrapolation to be ~ 0.2 MeV. Next, we estimate the systematic error of f_{D_s} due to the scaling violations, by performing the chiral extrapolation of $(f_{D_s} a) \sqrt{M_{D_s} a}$ in the lattice unit. Fitting the lattice data to NLO HMChPT (see the upper curve in Fig. 3) gives $\kappa = 0.0489(5)$ and $c_1 = 0.513(185)$ with $\chi^2/\text{dof} = 0.46$. At the

physical $M_\pi = 140$ MeV ($M_\pi a = 0.001842$), it gives $f_{D_s} a \sqrt{M_{D_s} a} = 0.0625(6)$. With the inputs $a^{-1} = 3.2418(56)$ GeV (in the chiral limit) and $M_{D_s} = 1968.50$ MeV, we obtain $f_{D_s} = 259.9(2.7)$ MeV. Thus we estimate the systematic error of f_{D_s} due to the scaling violations to be ~ 2.0 MeV. Again, assuming the discretization error to be ~ 2 MeV, together with the systematic errors due to the scaling violations and the chiral extrapolation, we obtain

$$f_{D_s} = 258.7 \pm 1.1 \pm 2.9 \text{ MeV}, \tag{25}$$

which is in good agreement with the experimental values [7,24, 25], as well as the experimental average $f_{D_s} = 257.5 \pm 4.6$ MeV [23].

Since the ratio f_{D_s}/f_D is expected to have systematic error less than those of f_D and f_{D_s}, our results of f_D and f_{D_s} yield

$$\frac{f_{D_s}}{f_D} = 1.2788 \pm 0.0264 \tag{26}$$

in good agreement with the experimental average $f_{D_s}/f_D = 1.258 \pm 0.038$ [23].

To summarize, we perform the first study of the masses and decay constants of the pseudoscalar D-mesons in two-flavors lattice QCD with domain-wall fermion, on the $24^3 \times 48$ lattice with lattice spacing $a \sim 0.062$ fm, for three sea-quark masses corresponding to the pion masses in the range 260–475 MeV. Our results of f_D (24), f_{D_s} (25) and their ratio (26), are all in good agreement with the experimental results, as well as with other lattice QCD results [26]. Since our calculation is done at one single lattice spacing, we cannot perform the extrapolation to the continuum limit. Nevertheless, we do not expect the combined systematic errors much larger than our estimates in (24) and (25), since the lattice spacing ($a \sim 0.062$ fm) is sufficiently fine, and our lattice action is free from $O(a)$ lattice artifacts. Likewise, since our calculation is done on a single volume, the finite volume effect cannot be estimated reliably. However, it is believed that the finite volume error of physical observables involving heavy (charm/bottom) quarks is smaller than other systematic ones. We will address these issues with calculations on different volumes as well as several lattice spacings. Moreover, to incorporate the internal quark loops of (u, d, s, c) quarks in our dynamical simulations, we are performing HMC simulations of $(2 + 1)$-flavors and $(2 + 1 + 1)$-flavors QCD on the $24^3 \times 48$ lattice, with the novel exact pseudofermion action for one-flavor DWF [27].

References

[1] K.G. Wilson, Phys. Rev. D 10 (1974) 2445.
[2] M. Creutz, Phys. Rev. D 21 (1980) 2308.
[3] D.B. Kaplan, Phys. Lett. B 288 (1992) 342;
    D.B. Kaplan, Nucl. Phys. B, Proc. Suppl. 30 (1993) 597.
[4] H. Neuberger, Phys. Lett. B 417 (1998) 141;
    R. Narayanan, H. Neuberger, Nucl. Phys. B 443 (1995) 305.
[5] T.W. Chiu, T.H. Hsieh, J.Y. Lee, P.H. Liu, H.J. Chang, Phys. Lett. B 624 (2005) 31.
[6] M. Artuso, et al., CLEO Collaboration, Phys. Rev. Lett. 95 (2005) 251801.
[7] M. Artuso, et al., CLEO Collaboration, Phys. Rev. Lett. 99 (2007) 071802.
[8] T.W. Chiu, et al., TWQCD Collaboration, Phys. Lett. B 651 (2007) 171.
[9] S. Duane, A.D. Kennedy, B.J. Pendleton, D. Roweth, Phys. Lett. B 195 (1987) 216.
[10] T.W. Chiu, Phys. Rev. Lett. 90 (2003) 071601;
     T.W. Chiu, Phys. Lett. B 716 (2012) 461.
[11] T.W. Chiu, T.H. Hsieh, Y.Y. Mao, TWQCD Collaboration, Phys. Lett. B 702 (2011) 131.
[12] T.W. Chiu, T.H. Hsieh, Y.Y. Mao, TWQCD Collaboration, Phys. Lett. B 717 (2012) 420.
[13] Y.C. Chen, T.W. Chiu, TWQCD Collaboration, Phys. Rev. D 86 (2012) 094508.
[14] T.W. Chiu, TWQCD Collaboration, J. Phys. Conf. Ser. 454 (2013) 012044.
[15] R. Narayanan, H. Neuberger, J. High Energy Phys. 0603 (2006) 064.
[16] M. Lüscher, J. High Energy Phys. 1008 (2010) 071.
[17] G. Colangelo, S. Durr, C. Haefeli, Nucl. Phys. B 721 (2005) 136.
[18] J. Beringer, et al., Particle Data Group Collaboration, Phys. Rev. D 86 (2012) 010001.
[19] S.R. Sharpe, Y. Zhang, Phys. Rev. D 53 (1996) 5125.
[20] A. Anastassov, et al., CLEO Collaboration, Phys. Rev. D 65 (2002) 032003.
[21] B.I. Eisenstein, et al., CLEO Collaboration, Phys. Rev. D 78 (2008) 052003.
[22] M. Ablikim, et al., BESIII Collaboration, Phys. Rev. D 89 (2014) 051104(R).
[23] J.L. Rosner, S. Stone, arXiv:1309.1924 [hep-ex].
[24] P. del Amo Sanchez, et al., BaBar Collaboration, Phys. Rev. D 82 (2010) 091103.
[25] A. Zupanc, et al., Belle Collaboration, J. High Energy Phys. 1309 (2013) 139.
[26] For a recent review, see, e.g., S. Aoki, Y. Aoki, C. Bernard, T. Blum, G. Colangelo, M. Della Morte, S. Durr, A.X.E. Khadra, et al., arXiv:1310.8555 [hep-lat];
     A.X. El-Khadra, PoS LATTICE 2013 (2013) 001.
[27] Y.C. Chen, T.W. Chiu, arXiv:1403.1683 [hep-lat].